

Grain size distributions for competitive growth with nucleation

R. Hilfer^{1,2} and P. Meakin³

¹ Department of Physics, University of Oslo, N-0316 Oslo, Norway

² Institut für Physik, Universität Mainz, Postfach 3980, W-6500 Mainz, Federal Republic of Germany

³ Experimental Station, DuPont de Nemours, Wilmington, DE 19880, USA

Received November 25, 1991

The paper introduces and discusses an idealized competitive growth model with nucleation for the microstructure formation during dense branching phase separation in thin Al/Ge films. Grain size and grain length distributions for the new model are obtained analytically and by simulation. These distributions exhibit a characteristic scaling form similar to cluster size distributions in many other growth models. The cutoff functions in these scaling forms and their influence on the determination of effective exponents are studied in detail. It is found that nucleation introduces a new length scale into the otherwise selfsimilar competitive growth model. This length scale appears only inside the cutoff function and diverges algebraically as the nucleation rate vanishes. We find both analytically and by simulation that the cutoff functions can exhibit stretched exponential behaviour $\sim \exp(-x^\alpha)$ for large arguments. Our analytical and simulation results for grain size and grain length distributions are in excellent quantitative agreement.

1. Introduction

A considerable interest in growth processes occurring far from equilibrium has developed in recent years. Such processes are commonly characterized by fractal geometries [1] and power law size distributions. These characteristics of nonequilibrium processes can often be understood in terms of scaling models. But in most cases the scaling forms are phenomenological and the scaling exponents cannot be calculated in a systematic fashion. Examples of the successful application of simple scaling ideas include the cluster size distribution in deposition processes (diffusion limited deposition [2, 3] and ballistic deposition [4]), the kinetics of cluster-cluster aggregation [5, 6] and the size distribution in fragmentation processes [7]. Because of the scientific and practical importance of such processes it is important to develop a better understanding

of the scaling laws that describe them. An important step in this direction is to study simple examples for which an analytical understanding can be obtained. Such an analytical description not only allows the quality and validity for familiar scaling models to be assessed but leads also to a better understanding of the role played by fluctuations in growth processes and how these fluctuations may influence fractal geometry, size distributions and growth kinetics.

Model studies such as the one presented here must be guided by experiment. Our experimental motivation stems from observations of growth in $\text{Al}_x\text{Ge}_{1-x}$ thin films. Such films exhibit an unusual growth morphology during phase separation from the amorphous into the crystalline state. A circular crystalline region grows from a nucleation center inside of which a branched, centered, dendritic structure of polycrystalline Ge embedded in monocrystalline Al is observed [8]. Many features of the unusual growth mode observed in the experiments have been approached theoretically by formulating and analysing a nonlinear moving boundary problem which gives a macroscopic description of the growth of the crystalline Al/Ge regions [9, 10]. The interesting features that have been explained in this way include the absence of the Mullins-Sekerka instability [9] for the circular growth shape as well as the linear growth law and the mechanism selecting the growth velocity.

Despite these encouraging results the theoretical approach has fallen short of a complete understanding mainly because the branched, poly-crystalline structure of the Ge-aggregate is left out of consideration. This is an important aspect if we want to understand the strongly temperature dependent length scale found in the experiment. A first step in this direction was taken in [11]. These authors studied diffusion limited aggregation (DLA) [13] with surface tension and nucleation. Surface tension leads to a finite finger width. But this finding is not relevant for systems with a dense branching morphology because upon renormalization the model still flows into the self-similar DLA fixed point [14–17]. Introducing nucleation

on the other hand allows us to study a new quantity, the grain size distribution, that might be relevant in the experimental system. For this reason we consider in the present paper a simple growth process with nucleation (but without branching) and try to extract a characteristic length scale from it.

Given the goal above we have chosen the simplest possible growth model, namely that of growing a flat surface by adding one layer after another. The only new ingredient is the possibility of nucleating new crystallites during the growth. We follow our previous work [11] on the more complicated DLA growth in the analysis of the resulting grain size distribution.

Let us assume for simplicity that grain ripening processes can be neglected. In other words temperature is considered to be so low that the grain structure resulting from growth process remains completely frozen, and there are no ripening processes of the microstructure on the time scale of the experiment.

2. Formulation of the model

The models used in this work employ a square lattice with a coordinate system whose axes are parallel to the diagonal directions of the squares. Each square represents a mesoscopic region of the size of a critical nucleus. The linear dimension of such a region is much smaller than the average crystallite but much larger than atomic dimensions.

The growth process consists of adding layers of squares to a base (initial) layer of width (lateral extent) W . The layers are taken to be parallel to one of the coordinate axes, say to the x -direction. At each step in the growth process a single layer of W squares is added. In this way a rectangular strip of width W is grown along the y -direction. Each square in the strip carries a number identifying the different "grains". Every grain carries a different number. Alternatively we can imagine the grains to be colored and the numbers would then identify different colors. With the addition of each new layer of squares each square receives its number according to the following specific growth and nucleation rules.

At the start of a simulation an initial layer is set up by assigning "color" numbers to all of the squares in it to represent the grain orientations. In actual simulations the last layer of a previous equilibration run can be used as the initial layer. A new layer of squares is then added. Each square in the added layer has two neighbours in the previous layer (called "parents"). The parent squares are defined as those squares that have a common edge with the squares in the added layer. A color number is assigned to each added square according to the following rules:

- a) With probability p_v , a new color number is chosen (i.e. a number not existing in all numbered squares).
- b) With probability $1 - p_v$, a color number is chosen according to the colors of the parent squares as follows:
 - if the two parent squares have identical colour numbers the same color is also assigned to the newly added square;

- if the two parent squares have different color numbers one of them is selected at random with probability $1/2$ as the color number for the new square.

In these models it is assumed that the nucleation probability p_v is the same for each nucleus in the added layer. In most simulations we employ a more realistic version in which we modify rule a) by distinguishing between nucleation probabilities p_v^g for grain boundaries (i.e. where the two parents have different colours) and p_v^f for free boundaries (i.e. when the parents belong to the same grain).

Each grain in this model originates with a nucleation event and the grain continues to grow as long as it remains part of the surface of the strip. The active growth surface of each grain increases or decreases as a result of the nucleation of new grains and the growth of competing grains. Thus the model represents a competitive growth model with nucleation as an additional "screening" mechanism.

We have been unable to find analytical solutions for this model in the general case where both p_v^f and p_v^g are nonzero. However for the case $p_v^f = 0$ exact analytical results have been obtained which will be presented below. In all other cases we have studied the model by computer simulation.

3. Simulations

In the simulations we generally distinguish three different cases: 1) no nucleation at free boundaries, i.e. $p_v^f = 0$, 2) no nucleation at grain boundaries, i.e. $p_v^g = 0$, and 3) equal nucleation probabilities at free boundaries and at grain boundaries, i.e. $p_v^g = p_v^f$.

The simulations were all performed for strips of width $W = 2500$ with periodic boundary conditions in the direction perpendicular to the growth direction of the strip. Starting from a single base layer we first grew 2000 to 10 000 layers to equilibrate the grain structure. After equilibration between 10 000 and 40 000 layers were added and used in the statistics obtained from one run. In most cases data from a single run were used.

Two different distributions are extracted from the simulation data. One is the grain size distribution $p_s(s)$, i.e. the probability density for finding a grain of size s . The second distribution, $p_l(l)$, is the probability density that a grain will have a length of l layers along the growth direction (here the y -axis).

3.1. Nucleation only at grain boundaries

Consider first the case $p_v^f = 0$ and $p_v^g = \nu$, i.e. nucleation occurs only at grain boundaries. In Fig. 1 we show a subregion of 100 by 100 squares from an actual simulation run. The zig-zag lines result from the choice of the coordinate system and represent the grain boundaries. For the texture shown in the figure the nucleation probability was $\nu = 0.1$. The resulting pattern is strongly anisotropic with grains elongated along the growth direction (y -axis). This effect increases with the grain size. Al-

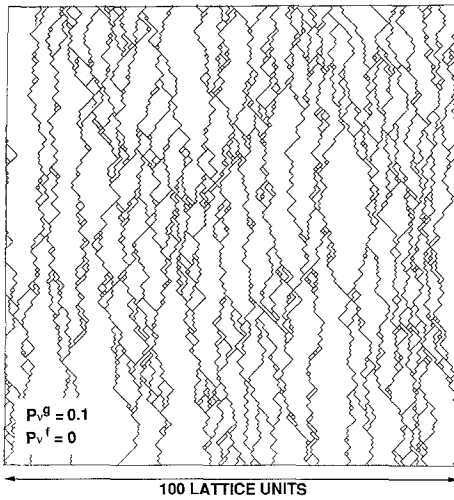


Fig. 1. Grain boundary configuration in a simulation of the grain boundary nucleation model with nucleation probability (p_v^g) of 0.1

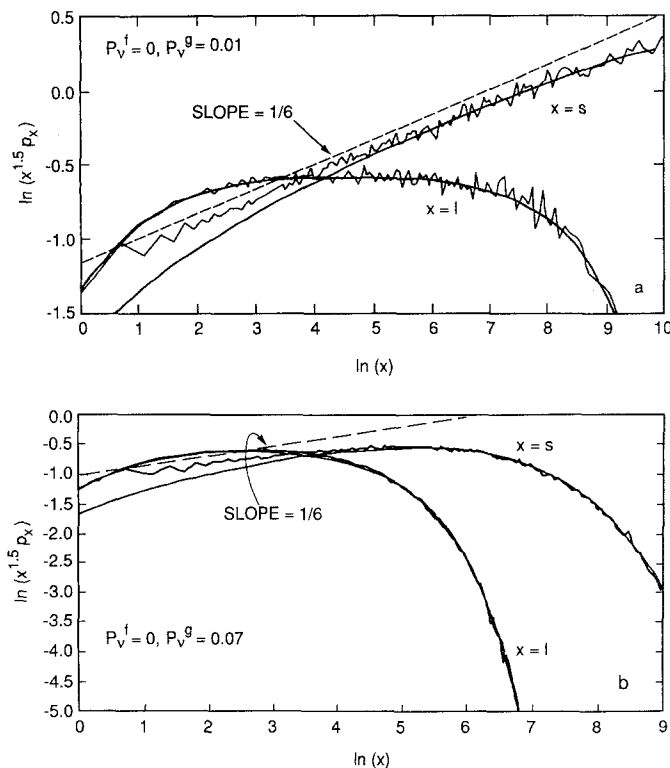


Fig. 2a, b. Grain length and grain size distributions of the grain boundary nucleation model. **a** shows the results for $p_v^g = 0.01$ and **b** for $p_v^g = 0.07$. The ragged curves are the simulation results, the smooth curves are the theoretical results. **a** has been drawn on the same scale as Figs. 5a and 7a to facilitate visual comparison

though a very wide distribution of sizes can be seen the distribution appears to be cut off at some large characteristic size. For larger values of ν this cutoff becomes even more apparent.

The existence of a cutoff in the grain size is confirmed by a study of the grain size distribution $p_s(s)$ and the grain length distribution $p_l(l)$. These two distributions are shown in Fig. 2 for the case where the nucleation

Table 1. Dependence of the parameters a_s , b_s , a_l and b_l in the size and length distribution functions $f_s(s)$ and $f_l(l)$ (3.2) on the nucleation probability (p_v^g) for the grain boundary nucleation model. The exponents are assumed to take their theoretical values

p_v^g	a_s	b_s	a_l	b_l
0.05	0.317	0.00472	0.590	0.00202
0.07	0.327	0.00795	0.610	0.00420
0.10	0.351	0.0176	0.645	0.00729
0.15	0.390	0.0396	0.671	0.0198
0.30	0.559	0.162	0.859	0.0866

probability is $\nu = 0.01$ and 0.07. In the figure we have plotted $\ln(l^{3/2} p_l(l))$ versus $\ln(l)$ as well as $\ln(s^{3/2} p_s(s))$ versus $\ln(s)$. For the case $\nu = 0.01$ the size distribution appears to follow a power law over almost three decades, while for the length distribution there is at best a range of about one decade if a power law regime exists at all. The scaling form

$$p_s(s) = s^{-\tau_s} f_s(s) \quad (3.1a)$$

appears to provide a satisfactory description of the size distribution $p_s(s)$ and we assume a similar form for the length distribution $p_l(l)$

$$p_l(l) = l^{-\tau_l} f_l(l). \quad (3.1b)$$

For most values of the nucleation probabilities ν (see Fig. 2b for example) (3.1a) was difficult to justify from the simulation data alone. We will see below however that it is justified by the theoretical analysis.

Next we tried to determine the form of the cutoff functions f_s and f_l . To this end we plotted the data in a semilogarithmic plot. We found that the cutoff function f_l seems to be well represented by an exponential function in the limit $l \rightarrow \infty$, suggesting the existence of a characteristic length scale. We also tested a stretched exponential form for the cutoff functions and found that this sufficiently improves the fits for the size distribution to justify the use of an additional parameter.

Consequently we assume that the cutoff functions are given generally are stretched exponentials, i.e.

$$f_s(s) = a_s \exp[-b_s s^{\beta_s}] \quad (3.2a)$$

and

$$f_l(l) = a_l \exp[-b_l l^{\beta_l}]. \quad (3.2a)$$

These forms for the cutoff functions will receive full justification in Sect. 4 below. The results from fitting to (3.2) are summarized in Table 1 for the parameter values $\nu = 0.05, 0.07, 0.1, 0.15$ and 0.3. Good fits to the data could always be obtained by using the values $\tau_s = 4/3$, $\beta_s = 2/3$, $\tau_l = 3/2$ and $\beta_l = 1$ suggested by theory.

From these fits we can tentatively conclude that the size distribution decays first as a power law with an exponent in the range 1.3...1.4, and is then cutoff exponentially at large sizes.

The data shown in Table 1 reveal another important aspect of the characteristic inverse sizes b_s and inverse

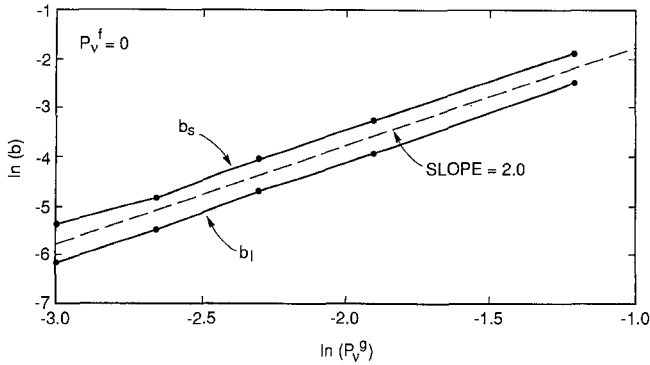


Fig. 3. The dependence of the cutoff parameters b_s and b_l for the grain size and grain length distributions (3.2a) and (3.2b) on the nucleation probability p_v^g for the grain boundary nucleation model

lengths b_l . Both of these quantities exhibit an algebraic dependence on the nucleation probability with an exponent of about 2.0. This is illustrated in Fig. 3 where the dependence of $\ln(b_s)$ and $\ln(b_l)$ on $\ln(\nu)$ is shown. Figure 3 corroborates the scaling forms of (3.1) and suggests that there exists a characteristic length scale introduced by the nucleation probability which diverges quadratically as the limit $\nu = 0$ is approached.

3.2. Nucleation only at free boundaries

In Fig. 4 we display the grain boundary texture obtained for the case $p_v^g = 0$ and $p_v^f = 0.1$. The texture is now very different from that shown in Fig. 1. While in Fig. 1 each grain was singly connected we find in the present case a nesting of grains inside grains. It is also evident that the nucleation mechanism is now much more efficient than before. Figure 4 shows a visibly smaller characteristic size than Fig. 1 while having the same value $\nu = 0.1$ of the nucleation probability. This is easy to understand. For the case of Fig. 1 a nucleation event occurred within each layer on average only at every tenth grain boundary square. In the present case however the nucleation occurs roughly after ten squares not counting squares adjacent to grain boundaries. Clearly this results in much more nucleation events per unit length than before. Figure 4 shows that it is still possible to deduce the growth direction from the anisotropy of the grains.

The grain size and grain length distributions for $\nu = 0.01$ and $\nu = 0.001$ are plotted in Fig. 5a and b. The fact that there is now a much smaller cutoff scale is immediately confirmed by these plots. Assuming again the scaling form of (3.1) we find exponents which are however larger in absolute value. Table 2 presents an overview of the results in the present case. It is seen that the effective power law exponents decrease systematically with increasing ν . This shows that the true power law scaling is still concealed by the cutoff function at such high values of ν . This might have been suspected from the small range of grain sizes visible in Fig. 4.

As the nucleation probability is lowered the power law regimes in p_s and p_l become larger and the effective exponents approach their asymptotic values. Figure 5b

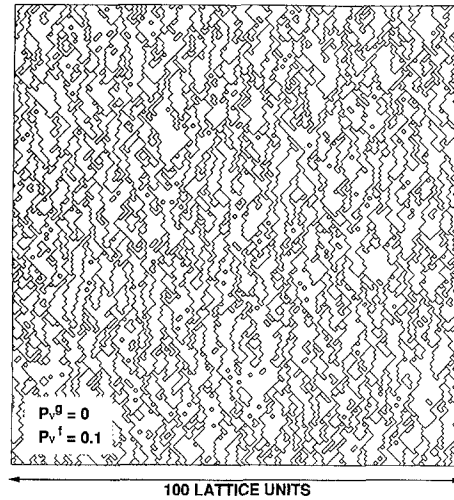


Fig. 4. A grain boundary configuration from a simulation of the free boundary nucleation model with nucleation probability $p_v^f = 0.1$

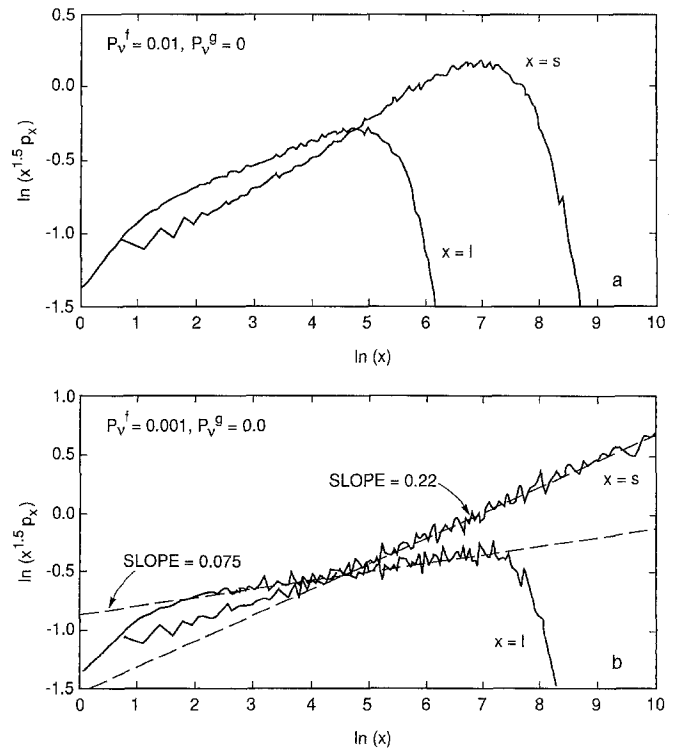


Fig. 5a, b. Grain length and grain size distributions from simulations of the free boundary nucleation model. **a** shows the results for $p_v^f = 0.01$ and **b** for $p_v^f = 0.001$. Figures 2a, 5a and 7a have been drawn on the same scale

Table 2. Effective values for the exponents τ_s and τ_l for the free boundary nucleation model ($p_v^g = 0$). A star, *, indicates no detectable power law regime

p_v^f	τ_l	τ_s
0.0003	1.45	1.32
0.001	1.42	1.28
0.003	1.40	1.25
0.010	1.34	1.22
0.030	1.26	1.22
0.100	*	1.17
0.300	*	1.03

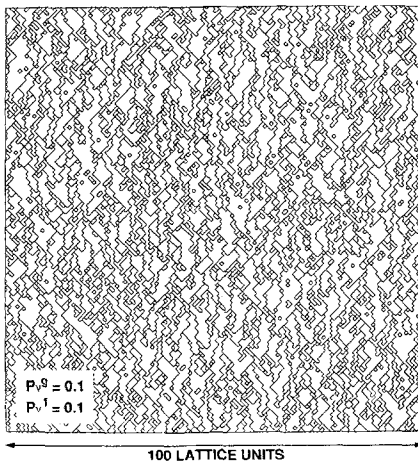


Fig. 6. A grain boundary configuration from a simulation of the symmetric nucleation model with nucleation probabilities $p_v^f = p_v^g = 0.1$

Table 3. Effective values for the length distribution exponent τ_l and the size distribution exponent τ_s for simulations with equal free boundary and grain boundary nucleation rates ($p_v^f = p_v^g = 0$). A star, *, indicates no detectable power law regime

ν	τ_l	τ_s
0.0003	1.47	1.32
0.001	1.43	1.32
0.003	1.41	1.28
0.010	1.36	1.27
0.030	*	1.25
0.070	*	1.28
0.150	*	1.29

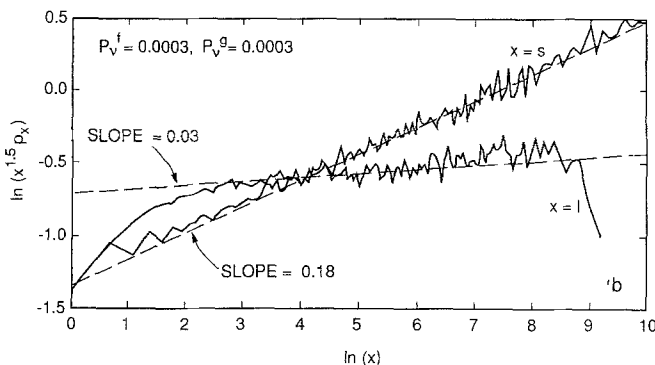
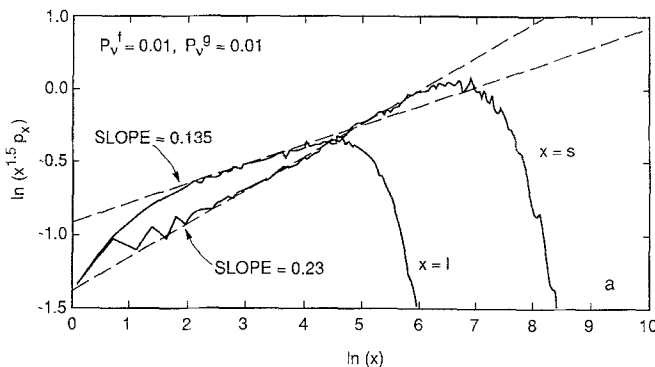


Fig. 7a, b. Grain length and grain size distributions from simulations of the symmetric nucleation model. **a** shows the results for $p_v^f = p_v^g = 0.01$ and **b** for $p_v^f = p_v^g = 0.0003$. Figures 2a, 5a and 7a have been drawn on the same scale

shows data for $p_v^f = 0.001$. The results collected in Table 2 and Fig. 5 are consistent with the idea that in the asymptotic limit $p_v^f \rightarrow 0$ the exponents τ_s and τ_l have the same values as in the grain boundary nucleation model.

3.3. Symmetric nucleation

The texture for the case $p_v^f = p_v^g = 0.1$ is shown in Fig. 6. The cutoff scale is even smaller because now the nucleation is most efficient, and on average a new grain is nucleated every ten squares.

The grain size distributions are shown again at two values of the nucleation probability. The results from fitting to the scaling forms are collected in Table 3 similar to the two previous cases. Again the simulation results are consistent with asymptotic values of 3/2 and 4/3 for τ_l and τ_s respectively.

4. Analytical treatment

The general model is too complicated to be solved analytically. But an exact analytical solution can be found for the case where $p_v^f = 0$ and $p_v^g = \nu$, (i.e. nucleation occurring only at grain boundaries with probability ν). This case becomes tractable if attention is focussed on the active surface length z of a single grain as a function of the number of added layers. The active surface length z of a grain is defined as the number of elementary squares touching the growth front. With each addition of a new layer the active surface of a grain can increase or decrease by one elementary square. The probabilities for these events are obtained from the rules of the algorithm as

$$\text{Prob}\{z \rightarrow z + 1\} = \frac{1}{4}(1 - \nu)^2$$

$$\text{Prob}\{z \rightarrow z\} = \frac{1}{2}(1 - \nu)^2 + \nu(1 - \nu)$$

$$\text{Prob}\{z \rightarrow z - 1\} = \frac{1}{4}(1 - \nu)^2 + \nu(1 - \nu) + \nu^2.$$

For example in the expression for $\text{Prob}\{z \rightarrow z - 1\}$ the first term gives the probability that z decreases if there is no nucleation at either one of the boundaries. The second term applies if there is nucleation at only one of the boundaries, and the third term describes grain nucleation at both boundaries. The other two cases are obtained similarly.

For a strip of width W the growth of a single grain always begins with an elementary square, i.e. initially $z = 1$, and stops when $z = 0$ for the first time. To calculate the grain size distribution or the grain length distribution we need to calculate the probability $g_{1,l}$ that a grain will have length l (i.e. the grain stops growing after adding l layers) if it started from a single nucleus (i.e. from $z = 1$). More generally if $g_{z,l}$ denotes the probability to find a grain of length l which started from an active surface z then $g_{z,l}$ obeys the equation

$$g_{z,l+1} = \frac{1}{4}(1 + \nu)^2 g_{z+1,l} + \frac{1}{2}(1 - \nu^2) g_{z,l} + \frac{1}{4}(1 - \nu)^2 g_{z-1,l} \quad (4.1)$$

with boundary values

$$g_{0,l} = g_{w,l} = 0 \quad (4.2a)$$

for $l \geq 1$ and

$$g_{0,0} = 1; \quad g_{z,0} = 0 \quad (4.2b)$$

for $0 < z \leq W$. Equations (4.1) and (4.2) can be solved using the method of generating functions [18]. Let

$$G_z(s) = \sum_{l=0}^{\infty} g_{z,l} s^l$$

denote the generating function for the probabilities $g_{z,l}$. The usual Ansatz $G_z(s) = [\beta(s)]^z$ gives the solution

$$G_z(s) = \frac{\beta_1^w \beta_2^z - \beta_1^z \beta_2^w}{\beta_1^w - \beta_2^w} \quad (4.3)$$

where

$$\begin{aligned} \beta_1(s) &= A_1 [1 + (1 - A_2)^{1/2}] \\ \beta_2(s) &= A_1 [1 - (1 - A_2)^{1/2}] \end{aligned} \quad (4.4)$$

and

$$\begin{aligned} A_1 &= \frac{2}{s(1-v)^2} - \frac{1+v}{1-v} \\ A_2 &= \left(\frac{2}{s(1+v)^2} - 1 \right)^{-2}. \end{aligned}$$

It can then be shown that the final result for the probability $g_{1,l}$ obtained from this solution reads

$$\begin{aligned} g_{1,l} &= \frac{1}{W} \frac{1-v}{1+v} (1-v^2)^l \\ &\times \sum_{i=1}^{w-1} \frac{\sin^2 \frac{\pi i}{W}}{1 + \cos \frac{\pi i}{W}} \left(\frac{1}{2} + \frac{1}{2} \cos \frac{\pi i}{W} \right)^l. \end{aligned} \quad (4.5)$$

This result shows that nucleation ($v \neq 0$) enters as an exponential prefactor to the sum representing the effect of the competitive growth process. Equation (4.5) is the exact result for the grain length distribution.

To understand the result better it is instructive to investigate the probabilities $g_{1,l}$ for large values of l . In the notation of Sect. 3 we have $p_l(l) = g_{1,l}$ for the probability density function. To calculate the asymptotic expansion of $p_l(l)$ for large l it is convenient to pass to a continuum of possible values for l by replacing the variable s in the generating function with $1/(1+u)$. To find the result equivalent to (4.5) the inverse Laplace-Transform is calculated with respect to u . This leads to Bessel-functions whose asymptotic expansion can then be utilized. We find the asymptotic result

$$p_l(l) \sim l^{-3/2} e^{-v^2 l} \quad (4.6)$$

for $l \rightarrow \infty$. Thus the grain length distribution exhibits a characteristic length scale l_0 given by

$$l_0 = b_l^{-1} = v^{-2} \quad (4.7)$$

which diverges quadratically as the nucleation probability goes to zero. This result agrees with the scaling forms of (3.1) and (3.2) and with the simulation data presented in Fig. 3. Similar behaviour, namely the existence of a characteristic length scale which diverges as a power law, was also observed in the diffusion limited aggregation model with nucleation [11].

Finally we turn to the distribution of grain sizes which we have not found exactly. Instead we calculate it from the exact result for the grain length distribution using the following argument. The random size S of a grain is given by $S = WL$ where L is the random length whose distribution has been calculated above, and W is the width. For the width we use the root mean square of the active surface during the growth, i.e. $W \sim (\langle z(l)^2 \rangle)^{1/2}$. We therefore have $W = BL^{1/2}$ for a grain whose random length is L . Therefore the grain size is given by $S = BL^{3/2}$. The probability density function $p_s(s)$ for the grain sizes now follows from $p_l(l)$ as

$$p_s(s) = \frac{2}{3} B^{-2/3} s^{-1/3} p(B^{-2/3} s^{-2/3}).$$

With this we find the result

$$\begin{aligned} p_s(s) &= \frac{2}{3W} \frac{1-v}{1+v} B^{-2/3} s^{-1/3} (1-v^2)^{(s/B)^{2/3}} \\ &\times \sum_{i=1}^{w-1} \frac{\sin^2 \frac{\pi i}{W}}{1 + \cos \frac{\pi i}{W}} \left(\frac{1}{2} + \frac{1}{2} \cos \frac{\pi i}{W} \right)^{(s/B)^{2/3}} \end{aligned} \quad (4.8)$$

with the asymptotic expansion

$$p_s(s) \sim s^{-4/3} e^{-v^2 (s/B)^{2/3}}. \quad (4.9)$$

The exponent for the power law decay has changed and the cutoff function is now a stretched exponential rather than a simple exponential as for the grain length distribution. The characteristic cutoff size s_0 again diverges quadratically as the nucleation probability v tends to zero.

$$s_0 = b_s^{-1} = v^{-2} B^{2/3}. \quad (4.10)$$

Again this result is in good agreement with the simulation data.

5. Discussion

In this section we reconsider the simulation results in the light of the analytical findings. Although 2.5×10^7 to 10^9 particles were aggregated for each parameter value the scale of the simulations presented here is moderate compared to those performed in ballistic deposition where as many as 10^{10} sites per run have been deposited using the

same computer resources (IBM 3090) as in this work, and as many as 10^{12} using a massively parallel machine [19].

We can use (4.5) to calculate the grain length distribution for the case displayed in Fig. 2. Note that (4.5) contains no adjustable parameter. The result is drawn as the solid line in Fig. 2. It is evident that the exact calculation and the simulation are nearly indistinguishable. This holds also for other values of the nucleation probability ν .

This result justifies the procedure used in Sect. 3 where we fitted the simulation data to scaling forms with exponents fixed at their theoretical values. In these fits the first 5 to 10 data points are usually discarded because the scaling forms of (4.6) and (4.9) apply only at larger values of l resp. s . The results for the grain boundary nucleation model are collected in Table 1. Note that the inverse cutoff length b_l is found close to the value expected from (4.7). This suggests that the parameter B can be determined by using the relation (4.10). We find that $\nu^2 b_s^{-1} = 0.57 \pm 0.05$ with 95% confidence so that $B \approx 0.43$.

We can now proceed to consider the grain size distribution. As noted above (4.7) for the grain size distribution is not an exact result. It involves the parameter B and cannot be expected to be accurate at small s . Using the value for B obtained above we obtain the fit displayed as the smooth curve in Fig. 2. While the deviations for small s had to be expected we again obtain good agreement as soon as $s > 50$. This shows that 1) the cutoff function is indeed a stretched exponential function and 2) that our determination of B is selfconsistent.

For the free boundary nucleation model and the symmetric nucleation model the effective exponents τ_s and τ_l are smaller than their asymptotic ($\nu \rightarrow 0$) values. This indicates that the cutoff functions $f_s(s)$ and $f_l(l)$ do not have the simple monotonically decreasing forms given in (3.2). However our results are consistent with (but do not strongly support) the idea that the distributions $p_s(s)$ and $p_l(l)$ can be described by (3.1) and (3.2) in the limit $\nu \rightarrow 0$.

All these results demonstrate that the cutoff functions are very important. We find that in general stretched exponential cutoffs can exist. Such cutoffs will only show a very slow crossover, and very large scale simulations are required to find the correct power law exponent, even

if it is known theoretically that power law behaviour is correct.

More importantly the comparison with the exact solution shows that the small size corrections are also important. In fact the true power law is found to appear only in an intermediate window. These difficulties increase the uncertainties in measuring the exponents τ_s and τ_l . The uncertainties are exacerbated if $p_\nu^f \neq 0$. In these cases the cutoff functions do not have a simple form and the uncertainties in determining τ_s and τ_l may be as large as 0.2 to 0.3. This is illustrated in Tables 2 and 3. Such difficulties appear to be characteristic for investigations of grain or cluster size distributions in simulation and experiment.

We thank Prof. H.E. Stanley for many discussions. One of us (R.H.) is grateful to the German Norwegian Research and Development Programme (Project B-2) for financial support.

References

1. Mandelbrot, B.B.: The fractal geometry of nature. New York: Freeman 1982
2. Racz, Z., Vicsek, T.: Phys. Rev. Lett. **51**, 2381 (1983)
3. Meakin, P.: Phys. Rev. A **27**, 1616 (1983)
4. Meakin, P.: J. Phys. A **20**, L1133 (1987)
5. Vicsek, T., Family, F.: Phys. Rev. Lett. **52**, 1669 (1984); Botet, R., Jullien, R.: J. Phys. A **17**, 2517 (1984); Kolb, M.: Phys. Rev. Lett. **53**, 1653 (1984); Friedlander, S.K.: Smoke dust and haze. New York: Wiley 1977
6. Meakin, P., Vicsek, T., Family, F.: Phys. Rev. B **31**, 564 (1985)
7. Cheng, Z., Redner, S.: Phys. Rev. Lett. **60**, 2450 (1988)
8. Deutscher, G., Lereah, Y.: Phys. Rev. Lett. **60**, 1510 (1988)
9. Alexander, S., Bruinsma, R., Hilfer, R., Deutscher, G., Lereah, Y.: Phys. Rev. Lett. **60**, 1514 (1988)
10. Hilfer, R.: In: Random fluctuations and pattern growth. Stanley, H.E., Ostrowsky, N. (eds.), p. 127. Dordrecht: Kluwer 1989
11. Hilfer, R., Meakin, P., Stanley, H.E., Trunfio, P.: (unpublished)
12. Mullins, W.W., Sekerka, R.F.: J. Appl. Phys. **34**, 232 (1963)
13. Witten, T.A., Sander, L.M.: Phys. Rev. Lett. **47**, 1400 (1981)
14. Meakin, P.: Phys. Rev. A **27**, 604 (1983)
15. Witten, T.A., Sander, L.M.: Phys. Rev. B **30**, 4093 (1984)
16. Meakin, P.: Ann. Rev. Phys. Chem. **39**, 237 (1988)
17. Halsey, T.C.: (unpublished)
18. Feller, W.: An introduction to probability theory and its applications. New York: Wiley 1968
19. Amar, J.G., Family, F.: Phys. Rev. Lett. **64**, 543 (1990)